International Journal of Bioinformatics and Computational Biology
2018; 3(1): 17-27
http://www.aascit.org/journal/ijbcb

AASCIT American Association for Science and Technology

In silico Analysis of Liriodenine as a Novel ATP-Competitive PIM1 Inhibitor in some Cancer Cell-Lines of Haematopoietic and Prostate Origins

Michael Aderibigbe Arowosegbe[1, 2, *], Olaposi Idowu Omotuyi[1], Oluwatosin Benedict Adu[2], Segun Adeola[2], Bimpe Folasade Ogungbe[2], Gabriel Eniafe[1], Oluwafemi Jude Ogunmola[3]

[1]Centre for Biocomputing and Drug Development, Adekunle Ajasin University, Akungba-Akoko, Ondo, Nigeria
[2]Department of Biochemistry, Lagos State University, Ojo, Lagos, Nigeria
[3]Department of Biology (Storage Technology), Federal University of Technology, Akure, Ondo, Nigeria

Email address

michael.a.arowosegbe@gmail.com (M. A. Arowosegbe)
[*]Corresponding author

Citation

Michael Aderibigbe Arowosegbe, Olaposi Idowu Omotuyi, Oluwatosin Benedict Adu, Segun Adeola[2], Bimpe Folasade Ogungbe, Gabriel Eniafe, Oluwafemi Jude Ogunmola. *In silico* Analysis of Liriodenine as a Novel ATP-Competitive PIM1 Inhibitor in some Cancer Cell-Lines of Haematopoietic and Prostate Origins. *International Journal of Bioinformatics and Computational Biology.* Vol. 3, No. 1, 2018, pp. 17-27.

Received: March 20, 2018; **Accepted**: April 2, 2018; **Published**: May 18, 2018

Abstract: PIM1–an oncogenic kinase–is overexpressed in a number of haematopoietic malignancies as well as solid tumors such as prostate cancer where it correlates with poor prognosis. Several studies have elucidated the roles of PIM1 in cell-cycle progression, cell survival, and tumourigenesis. Also, the distinctive characteristics of the ATP binding pocket of this kinase have been vividly reported. Thus, PIM1 is an attractive target for the design of selective pharmacological inhibitors. *In silico* methods were executed to investigate the non-ATP mimetic properties of liriodenine in comparison with the co-crystallized 9G5 and CX-4945, which are potent ATP-competitive PIM inhibitors. Consequently, the outcome of our study depicted the interactions of liriodenine with catalytic important aminoacyl residues in the ATP binding site of PIM1. Considering the ADME and cytotoxic parameters of the screened drug-like candidates together with CX-4945, we also showed that liriodenine displayed an improved probable ATP-competitive PIM1 inhibition when compared to CX-4945, a drug currently in Phase I/II clinical trials against cholangiocarcinoma. In the light of these findings, we put forward a valid argument, indicating that liriodenine can be preclinically/clinically researched as a potential targeted cancer therapy for haematopoietic malignancies as well as other solid tumours, most especially in prostate cancer.

Keywords: Haematopoietic Malignancies, Prostate, Inhibition, Liriodenine, PIM1, ADME

1. Introduction

The PIM (Proviral Integration site of mouse Moloney leukemia virus) family of serine/threonine kinase comprises three distinct kinases (PIM1, PIM2 and PIM3) and are highly conserved in multicellular organisms [1-2]. Each member is extremely homologous at the amino acid level but with different level of tissue distributions [3]. Yet, the functional redundancy among the three Pim kinases has been shown *in vitro* and *in vivo* [4-5]. Under physiological conditions, a number of tissues express PIM1 constitutively at low level [6]. However, PIM1 expression increases significantly in response to diverse growth factors, mitogens and cytokines, as it is regulated by different pathways such as ERG, JAK/STAT, hypoxia and NF-kBs [6-7]. PIM1 is also overexpressed in many human tumours, the elevated level of this kinase was first reported in leukemia and lymphoma tumours [1, 8]. Later, PIM1 was shown to be significantly upregulated in solid tumours, including prostate, pancreatic [9] and bladder cancers [1], advocating its participation in oncogenic processes in numerous cancer types. Obviously, PIM1 appears to contribute to cancer development in three major ways when it is overexpressed. Firstly, PIM1 inactivates Bad protein through the phosphorylation of Ser112, impeding the process of apoptosis [10]. Also, it can phosphorylate Cdc25A (G1/S), Cdc25C (G2/M), $p21^{CIP1/WAF1}$

and p27, which are all involved in the regulation of the cell cycle and the kinase promotes genomic instability [6]. In addition, Tursynbay *et al* [11] noted that PIM1 regulates drug resistance, senescence bypass, metastasis and epigenetic dynamics in various tumours. Therefore, PIM1 expression in hematopoietic malignancies and other tumour types corresponds with poor prognosis [12].

Other noteworthy oncogenic mechanisms of PIM kinases activities include: modulation of MYC transcriptional activity [13], regulation of cap-dependent translation [14], and pro-survival signaling, which thwarts the increased sensitivity of tumour cells to apoptosis [10]. PIM1 has therefore been proposed as an attractive target for anti-cancer drug development [15]. The following facts make PIM kinases typically attractive for pharmacological inhibition: (i) The phenotype of *PIM1* deficient mice is mild and non-lethal which might point to a favorable toxicity profile for PIM1 inhibitors [16]. (ii) The evidence of PIM inhibitor-based therapies has been noted where such inhibitions reduced the in vivo growths of xenograft leukemia and adenocarcinoma [17]. (iii) The ATP binding mode at the PIM binding site is significantly different compared to the majority of protein kinases [18]. The latter characteristics is principally interesting for drug design, encouraging the possibility for development of specific inhibitors [18].

PIM1 assumes a typical bi-lobed kinase fold structure with a deep cleft between the N- and C-terminal lobes connected via the hinge region (residues 123–125) [6, 18]. The N-terminal domain (residues 37–122) mainly comprises β-strands and a single α-helix whereas C-terminal domain (residues 126–305) is predominantly α-helical [18-19]. The ATP binding pocket of PIM1 kinase, situated between the two domains, is bordered by two loops: a glycine-rich G-loop (residues 44–52) and an activation A-loop (residues 185–204), and a hinge region. The distinctiveness of ATP binding in PIM1 is demonstrated in interactions inside the hinge region [6, 18]. Many protein kinases interact with ATP by forming two hydrogen bonds in hinge region [20]. The hinge region of PIM1 however lacks one of the canonical hydrogen bond donors within the backbone, containing a proline residue (Pro123) at the corresponding position [18]. Consequently, this unique feature also established the PIM1 protein kinase as an attractive target for drug design.

In this study, automatic docking was employed to determine the optimal positions and orientations of liriodenine, 10-Hydroxyliriodenine together with other ATP competitive PIM1 kinase inhibitors such as SMI-4a, TCS PIM-1 1, quercetagetin, PIM-1 inhibitor 2 and CX-4945 within the ATP binding pocket of PIM1 target. The binding affinity of each compound was compared to the docking score of the co-crystallized 9G5 in order to elucidate the hit identification and medicinal chemistry optimization. Consequently, the protein-ligand interactions of the lead compounds were analyzed using macromolecular visualization software packages such as PyMOL and VMD to identify the binding mode of each compound at the active site of PIM1. It has been indicated that early evaluation of ADME in the discovery phase decreases significantly the fraction of pharmacokinetics-related failure in the clinical phases [21-22]. Computer models have been endorsed as a rational alternative to experimental procedures for predicting ADME, especially at preliminary steps, when screened chemical structures are numerous but the availability of compounds is scarce [22-24]. Here, we used the new *in silico* SwissADME web-based tool to determine robust predictive models for physicochemical properties, drug-likeness and medicinal chemistry friendliness, among which in-house proficient methods such as the BOILED-Egg, iLOGP and Bioavailability radar were calculated. Furthermore, the experimental in vivo screening of anticancer drug-candidates through millions of natural and synthetic chemical compounds is relatively expensive and time-consuming. Nevertheless, different *in vitro* and *in silico* advancements in cell-based screening technologies have been proposed or developed to mitigate the cost of such screening and to unveil feasible mechanisms of the growth inhibition and killing of tumour cells [25]. Therefore, we evaluated the cytotoxicity of the drugable compounds against leukemia, lymphoma and prostate cancer cell-lines, using CLC-Pred, a computer-based web-service tool for virtual drug screening and an assessment of the selective cytotoxic effect of chemical compounds on cancer cell lines [25]. Finally, we demonstrated that liriodenine may serve as a potent ATP-competitive PIM1 inhibitor, leading to improved clinical outcome assessments of patients with a range of haematological malignancies and several solid tumours such as prostate cancer.

This work is aimed at providing *in silico* evidences, unveiling liriodenine as a potential selective ATP-competitive PIM1 inhibitor as compared to other selected PIM1 inhibitors in this study.

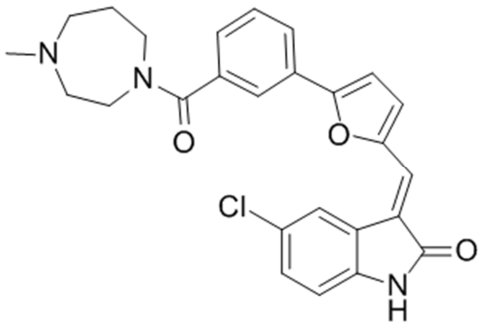

A

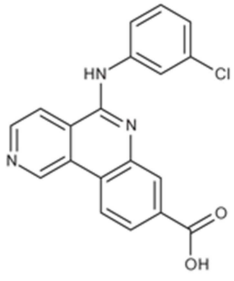

B

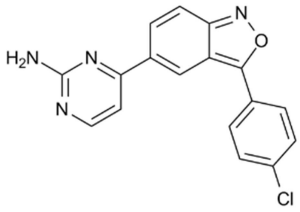

C

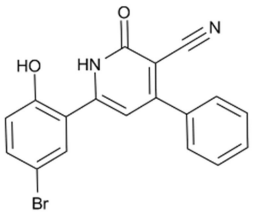

D

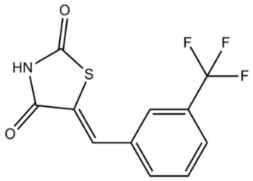

E

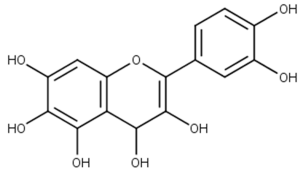

F

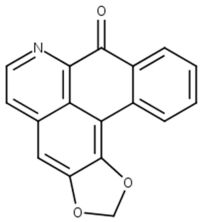

G

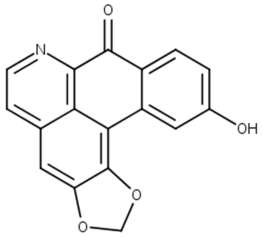

H

Figure 1. *The 2D chemical structure of A – co-crystallized 9G5 (CX-6258), B – CX-4945, C – PIM-1 inhibitor 2, D – TCS PIM-1 1, E – SMI-4a, F – quercetagetin, G – liriodenine, H – 10-hydroxyliriodenine.*

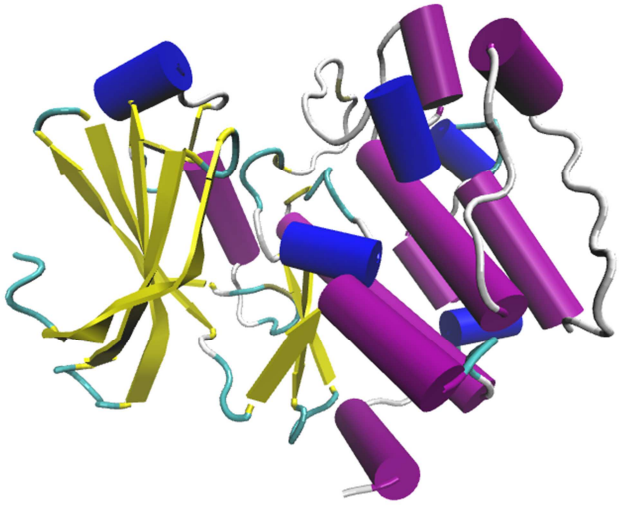

Figure 2. *3D structure of human PIM1 (pdb id: 5O13).*

2. Materials and Methods

2.1. Preparation of Ligands

The 2D chemical conformation of 10-Hydroxyliriodenine, CX-4945, liriodenine, PIM-1 inhibitor 2, quercetagetin, SMI-4a and TCS PIM-1 1 were downloaded from PubChem®, a popular database for the retrieval of ligands. Optimized ligands were docked into distinguished model using Ligand Fit theory in the MGL (Molecular Graphics Laboratory) Tools of AutoDock 4.2 version.

2.2. Preparation of Target

Crystal structure of PIM1 kinase in complex with small-molecule inhibitor 9G5 was retrieved from RCSB (Research Collaboratory for Structural Bioinformatics) protein data bank. The PDB ID of the kinase is 5O13. The structures were visualized using the Python-based PyMol® intended for the structural visualization of proteins. Water molecules, hetero atoms and the co-crystalized inhibitors were removed before executing docking simulations.

2.3. Molecular Docking

The pdqt file for each protein was generated using MGLTools of AutoDock 4.2 version. The protein target was treated as rigid body, while the rotatable bonds of the ligand were set to be free. The pre-calculated grid maps size was set at 60, 60, and 60 Å (x, y, and z) to include all the catalytic important amino acid residues and the spacing between grid points was 0.375 angstroms. The grid centre coordinates were exactly as that of the co-crystallized compounds in order to ensure that the ligands occupy the same binding pocket as obtained for PIM1 (5O13, 2.44 Å, x= -71.2, y= 47.01, z= -5.74). The time to dock each compound into the ATP binding site of the PIM1 was approximately 1-2 minutes. Docking simulations were executed on a HP workstation (Z800) with an intel Pentium D processor (3.06GHz).

2.4. ADME Scores and Bioavailability Radar Plot

The ADME (absorption, distribution, metabolism and excretion) properties for each lead compound was calculated using smile notation in Swiss ADME web-based tool [22]. Also, the bioavailability radar plot for liriodenine together with the co-crystallized 9G5 and the standard CX-4945 were depicted using the ADME web-based tool.

2.5. Protein-Ligand Complex Conformational Analysis

We complexed each lead compound (CX-4945 and liriodenine) and the co-crystallized 9G5 with PIM1 kinase separately in the pdb format using PyMol® and then submitted it on ProteinsPlus, an online server [26]. ProteinsPlus automatically generated the PoseView (2D) diagrams of the macromolecular complexes. In addition, another online server PLIP was applied to depict the 3-Dimensional conformation of each complex. The results were analyzed using macromolecular visualization software packages such as PyMol® and VMD®.

2.6. Cell-Line Cytotoxicity Prediction for Tumour Cells

The cytotoxic effects of the lead compounds on leukemia, lymphoma and prostate cancer cell-lines were predicted using a freely available web-service for cell-line cytotoxicity profile prediction (CLC-Pred: Cell-Line Cytotoxicity Predictor) in line with best practices in the early stages of drug development, drug repositioning and cancer research [25].

3. Results

3.1. The Binding Affinity as Calculated Using Molecular Docking Softwares

Molecular docking studies are essential to predict the most stable orientation of our chemical compounds when complexed with the target PIM1. Binding mode of a number of competitive inhibitors of PIM1 has been previously characterized, however, selectivity is still an issue not fully resolved at structural level [18, 27]. In this study, we explored the therapeutic inhibitory potentials of liriodenine in the ATP binding site of PIM1, a member of constitutively active calcium/calmodulin-regulated serine/threonine kinase family. We assessed the structural interactions of the lead compounds and the catalytic important amino acid residues in the binding sites of PIM1. In the results obtained for the molecular docking, the binding energy for liriodenine was better than other PIM1 inhibitors but the co-crystallized 9G5 showed the best docking score as depicted in table 1.

Table 1. *Docking Results for the Compounds.*

Compounds	Binding Energy (kcal/mol)
Co-crystallized 9G5	-11.3
10-Hydroxyliriodenine	-9.9
CX-4945	-10.6
Liriodenine	-10.9
PIM-1 inhibitor 2	-9.6
Quercetagetin	-8
SMI-4a	-8.6
TCS PIM-1 1	-10.2

3.2. Post Docking Analysis

A number of PIM1 kinase small molecule inhibitors are now at the pre-clinical research stage, development and testing [6]. Substantial efforts towards the design, discovery and development of clinically efficacious PIM1 inhibitors persist due to the significance of the target to cancer progression and its potential for novel selective inhibitors as drug candidates [28-29]. PIM1 take up a unique bi-lobed kinase fold structure with a deep cleft between the N- and C-terminal lobes connected by the hinge region (residues 123–125). The N-terminal domain (residues 37–122) mainly comprises β-strands and a single α-helix whereas C-terminal domain (residues 126–305) is predominantly α-helical [6, 18]. The ATP binding pocket of PIM1 kinase, situated between the two domains, is bordered by two loops: G-loop (residues 44–52) and an A-loop (residues 185–204), and a hinge region (residues 123–125). In this study, we compared the binding orientation of liriodenine with the co-crystallized 9G5 (CX-6258, an oxindole-based potent and selective PIM1 inhibitor) [18]. Liriodenine however was also benchmarked with standard CX-4945 (silmitasertib), an orally available casein kinase II (CK2α) inhibitor [30], which is also effectively inhibits PIM1 [31]. Obviously, it has been reported that CK2α and PIM1 are both constitutively active serine/threonine protein kinases involved in cell proliferation, differentiation and survival [18, 32]. The procedures were not only validation strategy, but also to provide insights into the efficacy of binding mode of our lead chemical structure at the ATP pocket of PIM1.

3.2.1. Binding Orientation of Co-crystallized 9G5 at the Catalytic Site of PIM1

In the PIM1–9G5 complex structure, we observed that the oxygen atom within the inhibitor oxindole donated a H-bond to amide H-atoms of side chain Lys67 residue as depicted by Figure 3 and 4, which has been previously reported by Bogusz and colleagues [18]. In addition, the hydroxy O-atom of the inhibitor was in H-bonding with the mainchain amine of Asp186 in the A-loop (Figure 4). However, it was noted from Figure 4 that the carbonyl oxygen formed a hydrogen interaction with amide H-atoms of Asp128, shredding the hydrophobic cleft as indicated in Figure 3. Also, we noted a π-stacking (parallel) interaction between the Phe49–which is situated in the backbone of the G-loop–and a furan moiety of 9G5, the interaction has been reported to stabilize the inhibitor in the ATP pocket. 9G5 is additionally stabilized in a hydrophobic pocket containing the sidechains in the N-terminal lobe of residues Val52 at the G-loop, Ala65 and Ile104, the C-terminal lobe Val126, Asp128 and Leu174, together with Ile185, which is situated in the A-loop of the

target. Moreover, it has been indicated that the binding orientation of the 9G5 roughly mimics the binding of adenine in the ATP pocket of PIM1 [18].

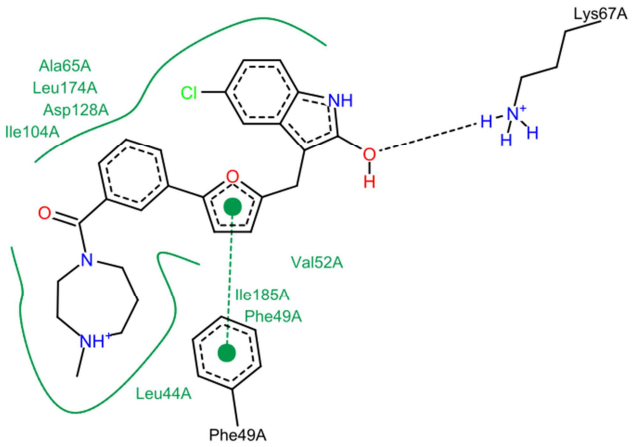

Figure 3. *The 2D representation of the interactions between co-crystallized 9G5 and the catalytic domains of PIM1, the black dashed lines indicate hydrogen bonds. The green solid lines show hydrophobic interactions and the green dashed line is the π-stacking interaction as created by PoseView.*

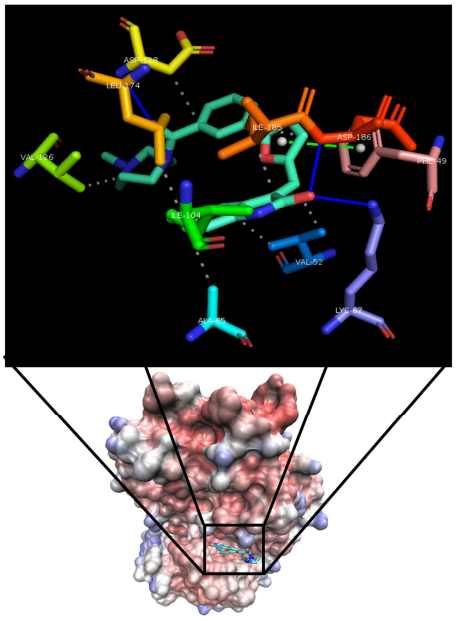

Figure 4. *The 3D protein-ligand profile for PIM1 and 9G5 interaction where the blue lines are the H-bonds, grey dashed lines show the hydrophobic interactions and green dashed line depicts the π-stacking (parallel) interaction.*

3.2.2. Binding Mode of CX-4945 at the ATP Pocket of PIM1

In the PIM1–CX-4945 complex structure, the carboxylate group of CX-4945 formed a salt bridge interaction with Lys67 (Figure 5 and 6), unlike the H-bond interaction which was depicted by Bogusz *et al*. Moreover, the inhibitor's carboxylate formed a H-bond with the amine of Asp186, as hitherto established [18], and Phe187 within the A-loop. A π-stacking (parallel) interaction between the Phe49 at the G-loop and the chlorophenyl moiety of CX-4945 was observed, which was similar to what we obtained for PIM1–9G5 complex. In addition, the significant hydrophobic components of the PIM1–CX-4945 interaction were contributed by the N-terminal lobe sidechains of Val52 at the G-loop, Ile104, Leu120 and the C-terminal lobe with sidechains Leu174 and Ile185 at the A-loop, as formerly illustrated by Bogusz and colleagues. In figure 5, the shredded hydrophobic patches might have been due to hydrogen bonding of the amide H-atom and the N-atoms of the heterocyclic ring of CX-4945 with either water molecules–which are not indicated in Figure 5 and 6–or other aminoacyl residues compared to what we saw with the co-crystallized 9G5.

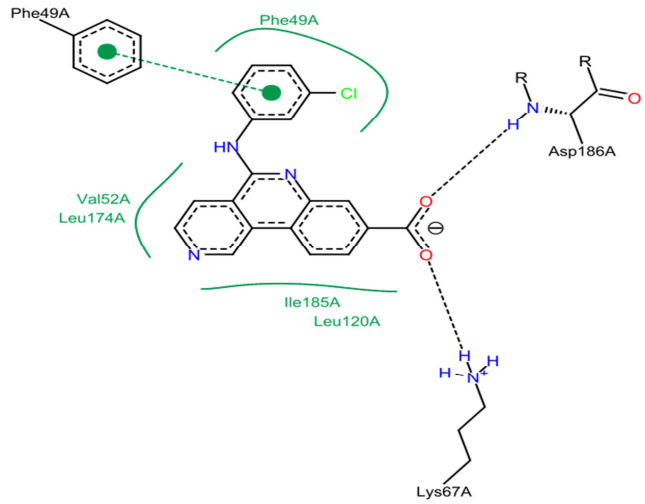

Figure 5. *The 2D representations of the interactions between CX-4945 and the catalytic domains of PIM1, the black dashed lines indicate hydrogen bonds or salt bridge interaction. The green solid lines show hydrophobic interactions and the green dashed line is the π-stacking interaction as created by PoseView.*

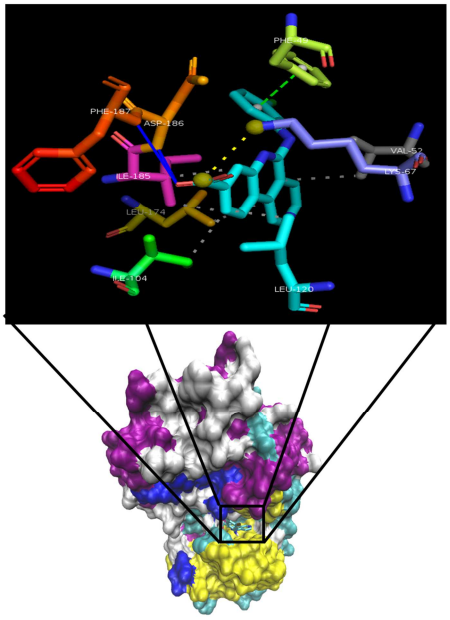

Figure 6. *The 3D protein-ligand profile for PIM1 and CX-4945 interaction where the blue lines are the H-bonds, grey dashed lines show the hydrophobic interactions, green dashed line depicts the π-stacking (parallel) and the yellow dashed line is the salt bridge interaction.*

3.2.3. Binding Interaction of Liriodenine in the ATP Site of PIM1

Liriodenine (8H-[1,3]benzodioxolo[6,5,4-de]benzo[g] quinolin-8-one), is an isoquinoline alkaloid widely distributed and acts as a chemotaxonomic marker in the Annonaceae family [33]. Also, it isolated from a plethora of other genera of plant species, such as *Fissistigma glaucescens* and *Liriodendron tulipifera* [34]. Studies have shown that liriodenine has prominent cytotoxic effects in several cancer cell lines, inducing DNA damage [34-35], reduced the expression of cyclin D1 and cyclin-dependent kinases [36] and decreased the phosphorylation of retinoblastoma protein in tumour cells [34], which led to G1/S phase arrest. Furthermore, the inhibitory effect upon DNA topoisomerase II together with the anti-proliferative and apoptosis-inducing actions of liriodenine have been presented as underlying therapeutic mechanisms [34, 37-38]. Hence, we were interested in investigating liriodenine as a potent and selective ATP competitive PIM1 inhibitor. In the PIM1–liriodenine complex structure, we noticed that the N-atom within the inhibitor liriodenine donated a H-bond to amide H-atoms of side chain Lys67 and Asp186 residues in Figure 7 and 8. However, a π-stacking (parallel) interaction between the Phe49 at the G-loop and any of the phenyl constituents of liriodenine as established for the co-crystallized 9G5 and the CX-4945 inhibitors was not depicted. The hydrophobic patches around the liriodenine were majorly contributed by the N-terminal lobe sidechains of Leu44, Phe49 and Val52 at the G-loop, Ile104, Leu120 and the C-terminal lobe with sidechain Ile185 at the A-loop, as formerly illustrated [18]. The shredded hydrophobic patches delineated in Figure 7 and 8 may be due to H-bonding of the carbonyl oxygen atoms and other O-atoms of the heterocyclic ring of liriodenine with either water molecules–which are not outlined in Figure 7 and 8 or other aminoacyl residues compared to what we saw with the co-crystallized 9G5.

Consequently, our study has shown that liriodenine mimics the same H-bond interaction with the catalytic-important Lys67 as compared to the co-crystallized 9G5. Although there was not salt bridge interaction in the PIM1-liriodenine complex, it was clearly observed that the amide of Asp186 was involved in H-bonding both in the liriodenine and CX-4945 complexed with PIM1. We also wish to hypothesize that the hydrophobic patches–surrounding the our lead chemical structure–are important in stabilizing liriodenine in the ATP binding pocket of PIM1 as previously reported (ref). Bogusz *et al* [18] noted that the binding of the furan moiety of 9G5 is mediated by hydrophobic interaction involving the sidechain of Phe49 and the backbone of the G-loop. Furthermore, they noted that the G-loop–which is partially distorted in some PIM1 structures–is stabilized by the hydrophobic interaction, mediated by Phe49 [18].

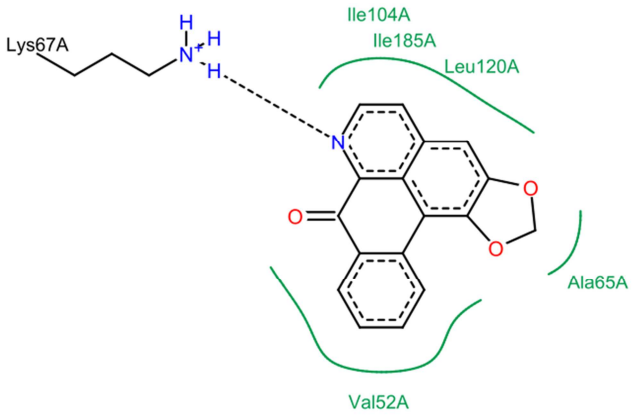

Figure 7. *The 2D representations of the interactions between liriodenine and the catalytic domains of PIM1, the black dashed lines indicate hydrogen bonds. The green solid lines show hydrophobic interactions as created by PoseView.*

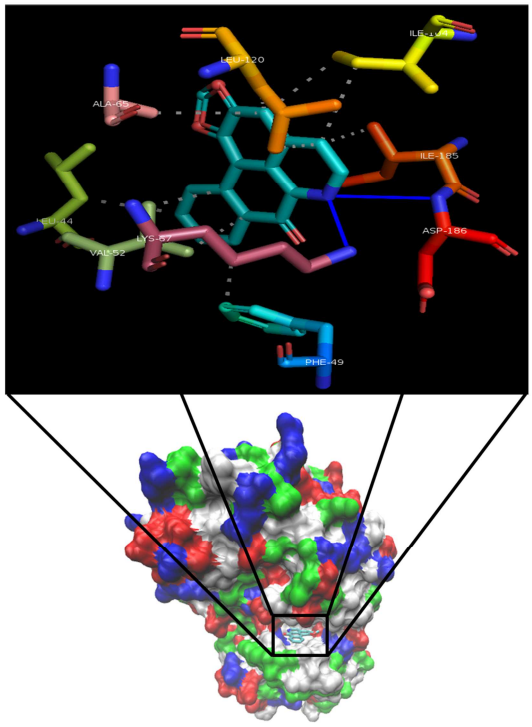

Figure 8. *The 3D protein-ligand profile for PIM1 and liriodenine interaction where the blue lines are the H-bonds and the grey dashed lines show the hydrophobic interactions.*

3.3. The Pharmacochemical Properties, Drug-Likeness and Medicinal Chemistry of Lead Structures

Computer models have been developed as a valid alternative to experimental procedures for prediction of ADME (Absorption, Distribution, Metabolism and Excretion). Indeed, this is noteworthily at initial steps, when they are plethora of investigated chemical structures but the compounds are not readily available [21-22]. The pioneer work of Lipinski [39] examined orally active compounds to explain physicochemical ranges for high probability to be an oral drug (i.e. the drug-likeness). This "Rule-of-five" shows

the relationship between pharmacokinetic and physicochemical parameters [21-22, 39]. In this study, we compared the physicochemical properties, drug-likeness and medicinal chemistry for the co-crystallized 9G5, CX-4945 and liriodenine as shown in Table 2 to 4. We have noted that the drug-like properties of liriodenine is satisfactorily comparable to the standard drug CX-4945, but significantly, the liriodenine was seen to be a more probable lead-like drug candidates as compared to the co-crystallized 9G5 and CX-4945 as shown by Table 2 to 4.

Table 2. *Physicochemical Properties of the Co-crystallized 9G5, CX-4945 and Liriodenine.*

Physicochemical Properties	Co-crystallized 9G5	CX-4945	Liriodenine
Formula	$C_{26}H_{24}ClN_3O_3$	$C_{19}H_{12}ClN_3O_2$	$C_{17}H_9NO_3$
Molecular weight	461.94 g/mol	349.77 g/mol	275.26 g/mol
Num. rotatable bonds	4	3	0
Num. H-bond acceptors	4	4	4
Num. H-bond donors	1	2	0
Molar Refractivity	140.59	98.56	76.67
TPSA	65.79 Å²	75.11 Å²	48.42 Å²

Table 3. *Drug-likeness of the Co-crystallized 9G5, CX-4945 and Liriodenine.*

Druglikeness	Co-crystallized 9G5	CX-4945	Liriodenine
Lipinski	Yes; 0 violation	Yes; 0 violation	Yes; 0 violation
Ghose	No; 1 violation: MR>130	Yes	Yes
Veber	Yes	Yes	Yes
Egan	Yes	Yes	Yes
Muegge	Yes	Yes	Yes
Bioavailability Score	0.55	0.56	0.55

Table 4. *Medicinal Chemistry of the Co-crystallized 9G5, CX-4945 and Liriodenine.*

Druglikeness	Co-crystallised 9G5	CX-4945	Liriodenine
PAINS	0 alert	0 alert	0 alert
Brenk	1 alert: michael acceptor 1	1 alert: Polycyclic aromatic hydrocarbon 3	0 alert
Leadlikeness	No; 2 violations: MW>350, XLOGP3>3.5	No; 1 violation: XLOGP3>3.5	Yes
Synthetic accessibility	3.83	2.43	2.77

3.3.1. Bioavailability Radar of the Lead Compounds

Bioavailability radar is plotted for a swift evaluation of drug-likeness [22]. Six physicochemical properties are taken into account for the co-crystallized 9G5, CX-4945 and liriodenine: lipophilicity, size, polarity, solubility, flexibility and saturation. The optimal range was depicted as a pink area within the radar plot. In our study, we discovered that the saturation parameter for liriodenine was lower than CX-4945, but the co-crystallized 9G5 showed optimal saturation among the compounds. However, other bioavailability parameters for liriodenine were better than the co-crystallized 9G5 and the drug standard CX-4945.

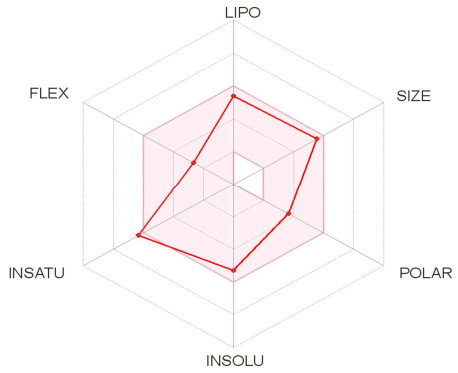

A

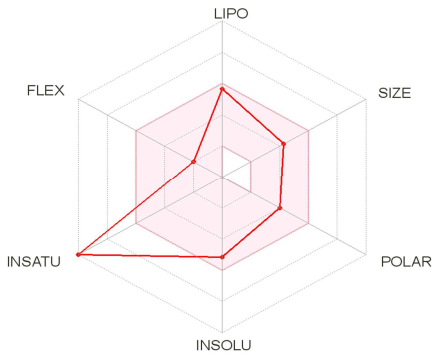

B

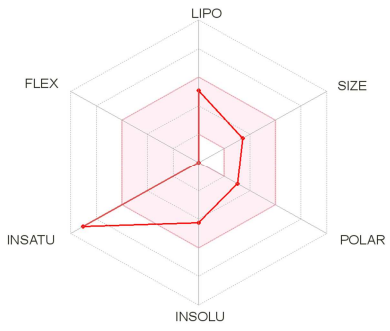

C

Figure 9. *The bioavailability radar for co-crystallized 9G5 (A), CX-4945 (B) and liriodenine (C), showing the lipophilicity (LIPO), size (SIZE), polarity (POLAR), solubility (INSOLU), flexibility (FLEX) and saturation (INSATU).*

3.4. *In silico* Cell-Line Cytotoxicity Prediction for Selected Tumour Cells

The combination of the computational assessment of the cytotoxic effect of chemicals in different cell-lines with the evaluation of the ligand-target interactions provides a more effective method for the design of new antineoplastic drugs [25]. In our study, we evaluated the cytotoxic effect of our compounds on cancer cell-lines from tissues such as the haematopoietic and lymphoid, together with blood tissues. Furthermore, we screened these compounds on DU-145 and PC-3, which are prostate cancer cell-lines [40-41]. Obviously, this was important since PIM1 is not only overexpressed in cancer of the leukemia and lymphoma tumours but also implicated in solid tumours such as prostate cancer [1, 8, 18]. Consequently, we compared the Pa (probability "to be active") values to Pi (probability "to be inactive") for the co-crystallized 9G5, CX-4945 and liriodenine. The Pa estimates the chances that the studied compound belongs to the sub-class of active compounds. However, the Pi calculates the chances that the studied compound belongs to the sub-class of inactive compounds. Although usually, there is no direct correlation between the Pa values and quantitative characteristics of activities of the compounds, this can help estimate the cytotoxic potentials of each chemical compounds. Clearly, the Pa > Pi for liriodenine is higher for most cancer cell-lines compared to the standard CX-4945 and the co-crystallized 9G5.

Table 5. *Cell-Line Cytotoxicity Predictor results for tumour cells by Co-crystallized 9G5.*

Pa	Pi	Cell-line	Cell-line name	Tissue/Organ
0.391	0.104	Kasumi 1	Childhood acute myeloid leukemia with maturation	Haematopoietic and lymphoid tissue
0.272	0.106	SR	Adult immunoblastic lymphoma	Haematopoietic and lymphoid tissue
0.098	0.009	MV4-11	Myeloid leukemia	Haematopoietic and lymphoid tissue
0.315	0.231	NALM-6	Adult B acute lymphoblastic leukemia	Haematopoietic and lymphoid tissue
0.073	0.072	TF-1	Bone marrow erythroleukemic	Haematopoietic and lymphoid tissue

Table 6. *Cell-Line Cytotoxicity Predictor results for tumour cells by CX-4945.*

Pa	Pi	Cell-line	Cell-line name	Tissue/Organ
0.388	0.033	RPMI-8226	Multiple myeloma	Haematopoietic and lymphoid tissue
0.295	0.041	KARPAS-299	Anaplastic large cell lymphoma	Haematopoietic and lymphoid tissue
0.350	0.144	NALM-6	Adult B acute lymphoblastic leukemia	Haematopoietic and lymphoid tissue
0.225	0.041	Jurkat	Acute leukemic T-cells	Blood
0.274	0.096	K562	Erythroleukemia	Haematopoietic and lymphoid tissue
0.275	0.132	C8166	Leukemic T-cells	Blood
0.259	0.120	MOLT-4	Acute T-lymphoblastic leukemia	Blood
0.249	0.131	PC-3	Prostate carcinoma	Prostate
0.303	0.190	Kasumi 1	Childhood acute myeloid leukemia with maturation	Haematopoietic and lymphoid tissue
0.213	0.120	Raji	B-lymphoblastic cells	Haematopoietic and lymphoid tissue
0.236	0.154	SR	Adult immunoblastic lymphoma	Haematopoietic and lymphoid tissue
0.162	0.109	Ramos	Burkitts lymhoma B-cells	Blood
0.225	0.179	H9	T-lymphoid	Haematopoietic and lymphoid tissue
0.184	0.139	CCRF-CEM	Childhood T acute lymphoblastic leukemia	Blood

Table 7. *Cell-Line Cytotoxicity Predictor results for tumour cells by Liriodenine.*

Pa	Pi	Cell-line	Cell-line name	Tissue/Organ
0.491	0.022	DU-145	Prostate carcinoma	Prostate
0.337	0.018	C8166	Leukemic T-cells	Blood
0.381	0.064	NALM-6	Adult B acute lymphoblastic leukemia	Haematopoietic and lymphoid tissue
0.370	0.055	HL-60	Promyeloblast leukemia	Haematopoietic and lymphoid tissue
0.301	0.089	RPMI-8226	Multiple myeloma	Haematopoietic and lymphoid tissue
0.258	0.048	Raji	B-lymphoblastic cells	Haematopoietic and lymphoid tissue
0.263	0.113	H9	T-lymphoid	Haematopoietic and lymphoid tissue
0.116	0.005	CCRF-SB	Childhood T acute lymphoblastic leukemia	Blood
0.070	0.007	RPMI 8402	Pre-T-lymphoblastoid cells. acute lymphoblastic leukemia	Haematopoietic and lymphoid tissue
0.146	0.095	ADR5000	Childhood T acute lymphoblastic leukemia	Blood
0.093	0.008	U-87 MG	Lymphoblastic lymphoma	Blood
0.211	0.185	MOLT-4	Acute T-lymphoblastic leukemia	Blood
0.056	0.045	MT4	Adult T acute lymphoblastic leukemia	Blood

4. Discussion

PIM1 is a member of constitutively active calcium/calmodulin-regulated serine/threonine kinase family [42]. This oncogenic kinase is primarily involved in transcriptional activation and cellular signal transduction pathways related to cell cycle progression and apoptosis [10, 43]. PIM1 is overexpressed in range of haematological malignancies and several solid tumours such as squamous cell carcinoma, prostate cancer, gastric carcinoma, and bladder cancer [1, 8-9]. Previous studies have shown that this

oncogene phosphorylates a number of cell cycle regulators such as Cdc25A (G1/S), Cdc25C (G2/M), $p21^{CIP1/WAF1}$ and p27 [6, 43]. Also, the kinase inactivates Bad protein through the phosphorylation of Ser112, impeding the process of apoptosis [10]. A plethora of PIM1 inhibitors have been reported in the recent years [44-45]. Although these inhibitors differ in their chemical structures, they all target the ATP binding site of PIM, which is between the hinge region, the A-loop and the G-loop [18].

PIM inhibitors are majorly grouped into three classes, due to the mechanistic mode of interaction with the kinase [18]. ATP-mimetic inhibitors replicate the interaction of ATP molecule with Glu121 in the hinge region of PIM1 [44, 46]. In addition, the non-ATP mimetics are described by their interaction with Lys67, a residue critical for sustaining the catalytically active state of PIM1, which forms a salt bridge with Glu89 [18, 47]. The third class of inhibitors satisfy both the above interactions [18]. Based on findings on staurosporine, a prototype inhibitor of a wide range of protein kinases, a greater number of reported PIM1 inhibitors belong to ATP-mimetics [12, 18]. Unfortunately for drug development, this class is characterized by a broad kinase inhibitory profile [18]. Since non-ATP-mimetics do not interact with the residues at the conserved hinge region among kinases–but rather with unique residues at the opposite side of the binding pocket for particular kinases–these inhibitors tend to be more selective [48-49].

The search for new anticancer compounds requires enormous effort in terms of manpower and cost. This effort emerges from the large number of compounds that need to be synthesized and subsequently biologically evaluated. Therefore, pharmaceutical industries have applied theoretical methods that enable the rational design of therapeutic agents [50-51]. Over a decade, bioinformatics has greatly evolved due to the development of specialized software, web-based tools as well as the increasing computer power [52]. For this reason, we have employed sophisticated *in silico* methods to predict the ATP-competitive, non-ATP-mimetic characteristics of liriodenine as compared to the co-crystallized 9G5 and CX-4945.

In the PIM1–liriodenine complex–like 9G5 and the standard CX-4945–liriodenine formed hydrogen bonds with the sidechain amine of Lys67. Furthermore, another H-bond was observed with the mainchain amine of Asp186 as compared to 9G5–like what was reported by Bogusz and colleagues–and CX-4945. These Lys67 and Asp186-mediated interactions are important for maintaining the constitutively active conformation of PIM1 by forming a number of polar interactions which stabilize the activation loop as reported by Bogusz *et al* [18]. We noted that the π-stacking (parallel) interaction between the Phe49–which is situated in the backbone of the G-loop–and a furan moiety of 9G5 was not present in the PIM1-liriodenine complex. We hypothesize that this might have led to the reduced binding affinity observed for liriodenine, since the interaction has been reported to stabilize the inhibitor in the ATP pocket [18]. Also, Ogawa and colleagues [53] has shown that Asp128 is an essential aminoacyl residue in the binding site, together with Lys67 and Phe46, which corroborate the findings from Bogusz *et al* [18]. The hydrophobic patches around the liriodenine were majorly contributed by the N-terminal lobe sidechains of Leu44, Phe49 and Val52 at the G-loop, Ile104, Leu120 and the C-terminal lobe with sidechain Ile185 at the A-loop, as formerly illustrated for 9G5 and CX-4945 by Bogusz *et al*.

Furthermore, early evaluation of ADME in the discovery phase reduces extremely the fraction of pharmacokinetics-related failure in the clinical phases [21-22]. We have noted that the drug-like properties–using web-based tools–of liriodenine is satisfactorily comparable to the standard drug CX-4945, but significantly, the liriodenine was seen to be a more probable lead-like drug candidates as compared to the co-crystallized 9G5 and CX-4945. Thus, our study will inspire the *in vitro* and *in vivo* evaluation of the inhibitory potency of liriodenine on the post translational PIM1.

Finally, since the screening of anticancer drug-candidates can be expensive and time-consuming, there is a clear need for computer-based tools for virtual drug screening and an evaluation of the selective cytotoxic effect of chemical compounds on cancer cell lines [25]. Early findings indicate the strong potential of liriodenine as a therapeutic agent for various types of cancers [33-38]. Therefore, our choice to investigate the cytotoxic effects of liriodenine on the selected cancer cell-lines is not out of place. Although there is no direct correlation between the Pa values and quantitative characteristics of activities of the compounds, the Pa > Pi for liriodenine for most of the cancer cell-lines shows that this inhibitor can be preclinically evaluated and clinically characterized as a effective targeted therapy for haematopoietic malignancies as well as other solid tumours, most especially in prostate cancer.

5. Conclusion

Our *in silico* evaluation of liriodenine has provided evidences for its non-ATP mimetic inhibitory properties. Hence, this study could inspire more *in vitro* and *in vivo* elucidations of liriodenine as a potential inhibitor against the oncogenic kinase activities of PIM1, overexpressed in numerous types of malignancies.

Acknowledgements

We acknowledges the training and technical support received from researchers at the Centre for Biocomputing and Drug Development, Adekunle Ajasin University, Akungba-Akoko, Ondo State, Nigeria.

Abbreviations

PIM1:	Provirus Integration site for Moloney leukemia virus 1 Kinase
9G5:	(E-5-chloro-3-((5-(3-(4-methyl-1,4-diazepane-1-carbonyl)phenyl)furan-2-yl)methylene)indolin-2-one)
CX-4945:	(5-((3-chlorophenyl)amino)benzo[c][2,6]naphthyridine-8-carboxylic acid)

References

[1] Grassow MN, Aparicio CB, Cecilia Y, Perez M, Galvan SM, Cañamero M, Renner O, Carnero A; Pim1 kinase cooperates with hormone treatment to promote bladder and ureteral urothelial hyperplasia. *Journal of carcinogenesis & mutagenesis* (2014) 5: 161.

[2] Drygin D, Haddach M, Pierre F, Ryckman DM: Potential use of selective and nonselective pim kinase inhibitors for cancer therapy. *Journal of medicinal chemistry* (2012) 55: (19), 8199-8208.

[3] Liu, Z, He W, Gao J, Luo J, Huang X, Gao C: Computational prediction and experimental validation of a novel synthesized pan-pim inhibitor PI003 and its apoptosis-inducing mechanisms in cervical cancer. *Oncotarget* (2015) 6: (10), 8019–8035.

[4] Grassow MN, Aparicio CB, Carnero A: The pim family of serine/threonineKinases in cancer. *Medicinal research reviews* (2014) 34: 1, 136–159.

[5] Brault L, Gasser C, Bracher F, Huber K, Knapp S, Schwaller J: Pim serine/threonine kinases in the pathogenesis and therapy of hematologic malignancies and solid cancers. *Haematologica* (2010) 95: 1004-1015.

[6] Liang C, Li Y: Use of regulators and inhibitors of Pim-1, a serine/threonine kinase, for tumour therapy (Review). *Molecular medicine report* (2014) 9: 2051-2060.

[7] Haddach M, Michaux J, Schwaebe MK, Pierre F, O'brien SF, Borsan C, Tran J, Raffaele N, Ravula S, Drygin D, Siddiqui-Jain A, Darjania L, Stansfield R, Proffitt C, Macalino D, Streiner N, Bliesath J, Omori M, Whitten JP, Anderes K, Rice WG, Ryckman DM: Discovery of cx-6258. a potent, selective, and orally efficacious pan-pim kinases inhibitor. *Acs medicinal chemistry letters* (2012) 3: 135−139.

[8] Kim J, Roh M, Abdulkadir SA: Pim1 promotes human prostate cancer cell tumorigenicity and c-MYC transcriptional activity. *BMC Cancer* (2010) 10: 248.

[9] Xu J, Zhnag T, Wang T, You L, Zhao Y: Pim kinases: an overview in tumors and recent advances in pancreatic cancer. *Future oncology* (2014) 10: 5.

[10] Gu J J, Wang Z, Reeves R, Magnuson N S: Pim1 phosphorylates and negatively regulates ask1-mediated apoptosis. *Oncogene* (2009) 28: 4261–4271.

[11] Tursynbay Y, Zhang J, Li Z, Tokay T, Zhumadilov Z, Wu D, Xie Y: Pim-1 kinase as cancer drug target: an update (Review). *Biomedical reports* (2016) 4: 140-146.

[12] Magnuson NS, Wang Z, Ding G, Reeves R: Why target pim1 for cancer diagnosis and treatment? *Future oncology* (2010) 6: 9.

[13] Horiuchi D, Camarda R, Zhou AY, Yau C, Momcilovic O, Balakrishnan S, Corella AN, Eyob H, Kessenbrock K, Lawson DA, Marsh LA, Anderton BN, Rohrberg J, Kunder R, Bazarov AV, Yaswen P, McManus MT, Rugo HS, Werb Z, Goga A: Pim1 kinase inhibition as a targeted therapy against triple-negative breast tumors with elevated myc expression. *Nature medicine* (2016) 22: 1321–1329.

[14] Nawijn MC, Alendar A, Berns A: For better or for worse: the role of pim oncogenes in tumorigenesis. *Nature reviews cancer* (2011) 11: 23–34.

[15] Xie, Y, Xie, Y: Pim1 kinase as a promise of targeted therapy in prostate cancer stem cells (Review). *Molecular and clinical oncology* (2016) 4: 13-17.

[16] Nakano H, Hasegawa T, Kojima H, Okabe T, Nagano T: Design and synthesis of potent and selective pim kinase inhibitors by targeting unique structure of atp-binding pocket. *ACS Medicinal chemistry Letters* (2017) 8 (5): 504–509.

[17] Zhao W, Qiu R, Li P, Yang J: Pim1: a promising target in patients with triple-negative breast cancer. *Medical oncology* (2017) 34: 142.

[18] Bogusz J, Zrubek K, Rembacz KP, Grudnik P, Golik P, Romanowska M, Wladyka B, Dubin G: Structural analysis of pim1 kinase complexes with atp-competitive inhibitors. *Scientific reports* (2017) 7: 13399.

[19] Mukaida N, Wang Y, Li Y: Roles of pim‐3, a novel survival kinase, in tumorigenesis. *Cancer science* (2011) 102 (8): 1437-1442.

[20] Garuti L, Roberti M, Bottegoni G: Non-atp competitive protein kinase inhibitors. *Current medicinal chemistry* (2010) 17 (25): 2804-2821 (18).

[21] Richmond W, Wogan M, Isbell J, Gordon WP: Interstrain differences of in vitro metabolic stability and impact on early drug discovery. *Journal of pharmaceutical sciences* (2010) 99 (11): 4463-4468.

[22] Daina A, Michielin O, Zoete V: Swissadme: a free web tool to evaluate pharmacokinetics, drug-likeness and medicinal chemistry friendliness of small molecules. *Scientific reports* (2017) 7: 42717.

[23] Paula da Silva CHT, Barreto da Silva V, Resende J, Rodrigues PF, Bononi FC, Benevenuto CG, Taft CA: Computer-aided drug design and admet predictions for identification and evaluation of novel potential farnesyltransferase inhibitors in cancer therapy. *Journal of molecular graphics and modelling* (2010) 6 (26): 513-523.

[24] Ntie-Kang F: An in silico evaluation of the admet profile of the StreptomeDB database. *SpringerPlus* (2013) 2: 353.

[25] Lagunin AA, Dubovskaja VI, Rudik AV, Pogodin PV, Druzhilovskiy DS, Gloriozova TA, Filimonov DA, Sastry NG, Poroikov VV: Clc-Pred: a freely available web-service for in silico prediction of human cell line cytotoxicity for drug-like compounds. *Plos one* (2018) 13 (1): e0191838.

[26] Fährrolfes R, Bietz S, Flachsenberg F, Meyder A, Nittinger E, Otto T, Volkamer A, Rarey M: Proteinsplus: a web portal for structure analysis of macromolecules. *Nucleic Acids Research* (2017).

[27] Kim W, Youn H, Kwon T, Kang J, Kim E, Son B, Yang HJ, Jung Y, Youn B: Pim1 kinase inhibitors induce radiosensitization in non-small cell lung cancer cells. *Pharmacological Research* (2013) 70 (1): 90-101.

[28] Fan R, Lu Y, Fang Z, Guo X, Chen Y, Xu Y, Lei Y, Liu K, Lin D, Liu L, Liu X: Pim-1 kinase inhibitor smi-4a exerts antitumor effects in chronic myeloid leukemia cells by enhancing the activity of glycogen synthase kinase 3β. *Molecular Medicine Reports* (2017) 16: 4603-4612.

[29] Sawaguchi Y, Yamazaki R, Nishiyama Y, Sasai T, Mae M, Abe A, Yaegashi T, Nishiyama H, Matsuzaki T: Rational design of a potent pan-pim kinases inhibitor with a rhodanine–benzoimidazole structure. *Anticancer Research* (2017) 37 (8): 4051-4057.

[30] Chandrika G, Mansi S, Sunil M, Malika K, Lidija P, Melanie H, Yali D, Chunhua S, Jonathon Lp, Bi-Hua T, Sinisa D: Casein kinase ii (ck2) as a therapeutic target for hematological malignancies. *Current Pharmaceutical Design* (2017) 23 (1): 95-107 (13).

[31] Cozza G, Sarno S, Ruzzene M, Girardi C, Orzeszko A, Kazimierczuk Z, Zagotto G, Bonaiuto E, Di Paolo ML, Pinna LA: Exploiting the repertoire of ck2 inhibitors to target dyrk and pim kinases. *Biochimica et Biophysica Acta (BBA) - Proteins and Proteomics* (2013) 1834 (7): 1402-1409.

[32] Koronkiewicz M, Chilmonczyk Z, Kazimerczuk Z, Orzeszko A: Deoxynucleosides with benzimidazoles as aglycone moiety are potent anticancer agents. *European Journal of Pharmacology* (2018) 620: 146-155.

[33] Nordin N, Majid NA, Hashim NM, Rahman MA, Hassan Z, Ali HM: Liriodenine, an aporphine alkaloid from *Enicosanthellum pulchrum*, inhibits proliferation of human ovarian cancer cells through induction of apoptosis via the mitochondrial signaling pathway and blocking cell cycle progression. *Drug Design Development and Therapy* (2015) 9: 1437–1448.

[34] Li L, Xu Y, & Wang B: Liriodenine induces the apoptosis of human laryngocarcinoma cells via the upregulation of p53 expression. *Oncology Letters* (2015) 9: 1121-1127.

[35] Chen C, Wu H, Chao W, Lee C: Review on pharmacological activities of liriodenine. *African Journal of Pharmacy and Pharmacology* (2013) 7 (18): 1067-1070.

[36] Chen C, Chen S, Chen C: Liriodenine induces g1/s cell cycle arrest in human colon cancer cells via nitric oxide- and p53-mediated pathway. *Process Biochemistry* (2012) 47 (10): 1460-1468.

[37] Chacón IC, González-Esquinca AR: Liriodenine alkaloid in Annona diversifolia during early development. *Natural Product Research* (2012) 26 (1): 42-49.

[38] Yao C, Cao X, Fu Z, Tian J, Dong W, Xu J, An K, Zhai L, Yu J: *Boschniakia rossica* polysaccharide triggers laryngeal carcinoma cell apoptosis by regulating expression of bcl-2, caspase-3, and p53. *Medical science monitor* (2017) 23: 2059 –2064.

[39] Lipinski CA: Lead- and drug-like compounds: the rule-of-five revolution. *Drug discovery today technologies* (2004) 1 (4): 337-341.

[40] Rybak AP, He L, Kapoor A, Cutz J, Tang D: Characterization of sphere-propagating cells with stem-like properties from du145 prostate cancer cells. *Biochimica et Biophysica Acta (BBA) - Molecular Cell Research* (2011) 1813 (5): 683-694.

[41] Samarghandian S, Afshari JT, Davoodi S: Chrysin reduces proliferation and induces apoptosis in the human prostate cancer cell line pc-3. *Clinics* (2011) 66 (6): 1073-1079.

[42] Maier CJ, Maier RH, Rid R, Trost A, Hundsberger H, Eger A, Hintner H, Bauer JW, Onder K: PIM-1 kinase interacts with the DNA binding domain of the vitamin D receptor: a further kinase implicated in 1,25-(OH)2D3 signaling. *BMC Molecular Biology* (2012) 13: 18.

[43] Morishita D, Katayama R, Sekimizu K, Tsuruo T, Fujita N: pim kinases promote cell cycle progression by phosphorylating and down-regulating p27kip1 at the transcriptional and posttranscriptional levels. *Cancer Research* (2008) 68 (13): 5076–85.

[44] Merkel AL, Meggers E, Ocker M: PIM1 kinase as a target for cancer therapy. *Expert Opinion on Investigational Drugs* (2012) 21 (4): 425-436.

[45] Arunesh GM, Ekambaram S, Krishna MH, Kumar JS, Viswanadhan: Small molecule inhibitors of PIM1 kinase: July 2009 to February 2013 patent update. *Expert Opinion on Therapeutic Patents* (2014) 24 (1): 5-17.

[46] Olla S, Manetti F, Crespan E, Maga G, Angelucci A, Schenone S, Bologna M, Botta M: Indolyl-pyrrolone as a new scaffold for pim1 inhibitors. *Bioorganic & Medicinal Chemistry Letters* (2009) 19 (5): 1512-1516.

[47] Silvia S, Cristina T, Maurizio B: Using Insights into Pim1 Structure to Design New Anticancer Drugs. *Current Pharmaceutical Design* (2010) 16 (35): 3964-3978 (15).

[48] Bullock AN, Russo S, Amos A, Pagano N, Bregman H, Debreczeni JE, Lee WH, von Delft F, Meggers E, Knapp S: Crystal structure of the pim2 kinase in complex with an organoruthenium inhibitor. Plos One (2009) 4 (10): e7112.

[49] Le BT, Kumarasiri M, Adams JRJ, Yu M, Milne R, Sykes MJ, Wang S: Targeting Pim kinases for cancer treatment: opportunities and challenges. *Future Medicinal Chemistry* (2015) 7 (1).

[50] Mohammad HB, Khurshid A, Sudeep R, Jalaluddin MA, Mohd A, Mohammad HS, Saif H, Mohammad AK, Ivo P, Inho C: Computer aided drug design: success and limitations. *Current Pharmaceutical Design* (2016) 22 (5): 572-581 (10).

[51] Hopkins AL: Network pharmacology: the next paradigm in drug discovery. *Nature Chemical Biology* (2008) 4: 682–690.

[52] Mingli X, Yu C, Wenjie F, Lijuan C, Yirong M: Computer-Aided Drug Design: Lead Discovery and Optimization. *Combinatorial Chemistry & High Throughput Screening* (2012) 15 (4): 328-337 (10).

[53] Ogawa N, Yuki H, Tanaka A: Insights from pim1 structure for anti-cancer drug design. *Expert Opinion on Drug Discovery* (2012) 7 (12): 1177-1192.